Article │ Received 30 January 2025; Accepted 23 March 2025; Published 28 March 2025
https://doi.org/10.55092/pe20250003

Experimental and numerical analysis of quasi-static compression behaviors of a novel ellipse-arc re-entrant honeycomb

Yuxin Tang[1,2], Yifeng Zhong[1,2]*, Minfang Chen[1,2], Rong Liu[1,2] and Yubo Gao[3]

[1] School of Civil Engineering. Chongqing University, Chongqing, China
[2] Key Laboratory of New Technology of Construction of Cities in Mountain Area (Chongqing University), Ministry of Education, Chongqing 400045, China
[3] School of Mechanical and Aerospace Engineering, Nanyang Technological University, Singapore

* Correspondence author; E-mail: zhongjy58@sina.com.

Abstract: This study aims to investigate the mechanical properties of a novel elliptic-arc re-entrant honeycomb (ERH) structure under quasi-static compression. Through a combination of experimental and numerical analysis methods, the mechanical response of the uni- and multi-cellular structure under compression is comprehensively analyzed. The experimental section employs precise instruments to conduct compression tests on the 3D-printing specimens with recording load-displacement curves and energy absorption characteristics. On the other hand, numerical analysis employs the finite element method to simulate the deformation and stress distribution within the honeycomb structure. The findings reveal that the novel ERH structure exhibits significant advantages in terms of load-bearing capacity and energy absorption efficiency, suggesting its practical applicability. This research not only highlights the superior performance of the new honeycomb structure but also offers valuable insights and methodologies for designing and optimizing lightweight, high strength materials essential for various engineering and industrial applications.

Keywords: elliptical-arc re-entrant honeycomb; experimental and numerical analysis; auxetic effect

1. Introduction

The honeycomb structure features a distinctive geometry and arrangement, comprising a two-dimensional in-plane array of units and a parallel out-of-plane stack [1]. These cellular structures demonstrate a range of unique properties, including exceptional compressive properties [2], high specific stiffness/specific strength [3], specific energy absorption [4], and distinctive acoustic energy absorption [5]. As a new negative Poisson ratio material, auxetic honeycomb structure has attracted extensive attention in the field of materials science and engineering due to its unique geometry and excellent mechanical properties [6,7].

Certain oval fruits like olives and persimmons possess outer shells with high strength and stiffness, capable of efficiently distributing stress during compression or impacts to resist extrusion and compression forces [8]. Drawing inspiration from the olive pit's shape, this study introduces a novel auxetic honeycomb structure by substituting the straight inclined struts with elliptic-arc struts in the re-entrant honeycomb design (Figure 1).

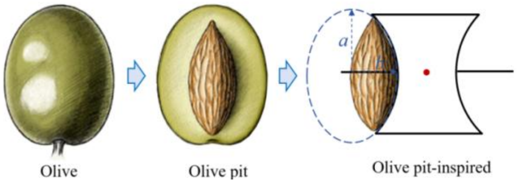

Figure 1. NPR honeycomb structure with elliptic-arc struts inspired by olive pit.

2. Geometrical description of the ERH

Inspired by the concepts of natural biological structures, an elliptic-arc re-entrant honeycomb (ERH) model based on a re-entrant auxetic honeycomb with negative Poisson's ratio is proposed. Different from conventional re-entrant honeycomb in Figure 2(a) or circular-arc re-entrant honeycomb in Figure 2(b), inclined struts are replaced by elliptic-arc struts (as shown in Figure 2(c). Elliptical arcs offer several advantages over circular arcs in terms of stress distribution, including more uniform stress distribution, higher load-bearing capacity, and greater adaptability, making them potentially advantageous in engineering structures, particularly when long-term stability and structural strength are key considerations.

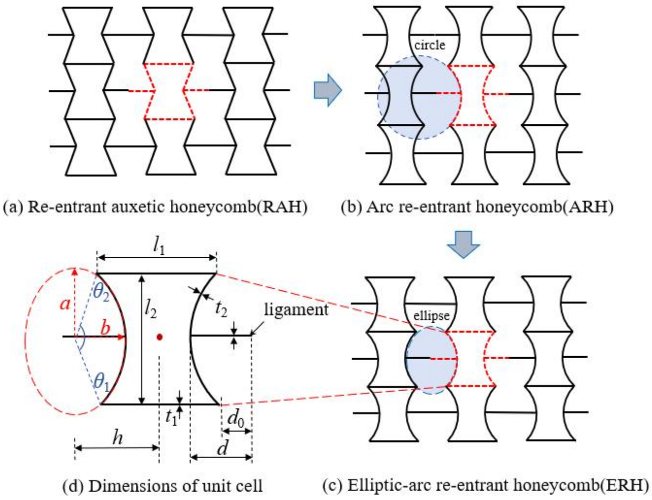

Figure 2. Geometry of **(a)** re-entrant auxetic honeycomb (RAH); **(b)** arc-shaped re-entrant honeycomb (ARH); **(c)** elliptic-arc re-entrant honeycomb (ERH); **(d)** dimensions of unit cell within the ERH.

Figure 2(d) presents the dimensions of the ERH's unit cell. Here, a and b represent the ellipse's major and minor axes, d is half-length of the horizontal ligament, d_0 is half- distance between adjacent unit cells, t_1 and t_2 represent the thicknesses of the horizontal and elliptic-arc struts, respectively; l_1 is the width of the cell; l_2 is the length of the horizontal strut, and h is the horizontal distance from the ellipse center to the geometric center of ERH. It is worth noting that all length measurements are referenced to the center axis of each strut.

3. Results and discussion

To investigate the quasi-static compression behaviors of ERH structures, the 3D-printed specimens were prepared by Fused Deposition Modeling (FDM) technology, utilizing ABS plastic as the printing material, with material properties determined from standard material properties test: elastic modulus of 2,319 MPa, Poisson’s ratio of 0.37, and density of 1.2 g/cm^3.

Figure 3 illustrates the arrangement of axial compression test and the geometries of uni- and 5×5 multi-cellular ERH specimens. The dimensions of these specimens are detailed in Table 1, where H, W and L denote the total height, width and length of the specimen, respectively. In the compression test, displacement loading control was employed with a loading rate of 2.0 mm/min. Pre-loading was conducted prior to the test to establish a steady state. The testing machine was connected to a computer to capture the applied load and displacement data obtained from the sensor. Compressive deformation mode was recorded using a digital Camera.

Table 1. Comparison of displacement modes of uni- and multi-cellular ERH in different stages predicted by 3D-EXP and 3D-FEM (unit: mm).

Parameters	l_1	l_2	t_1	t_2	d	d_0	H	W	D
uni-cellular	65	82	2	4	28	18	84	100	30
Multi-cellular	18.5	19	1	1.5	8.5	5.5	102	150	50

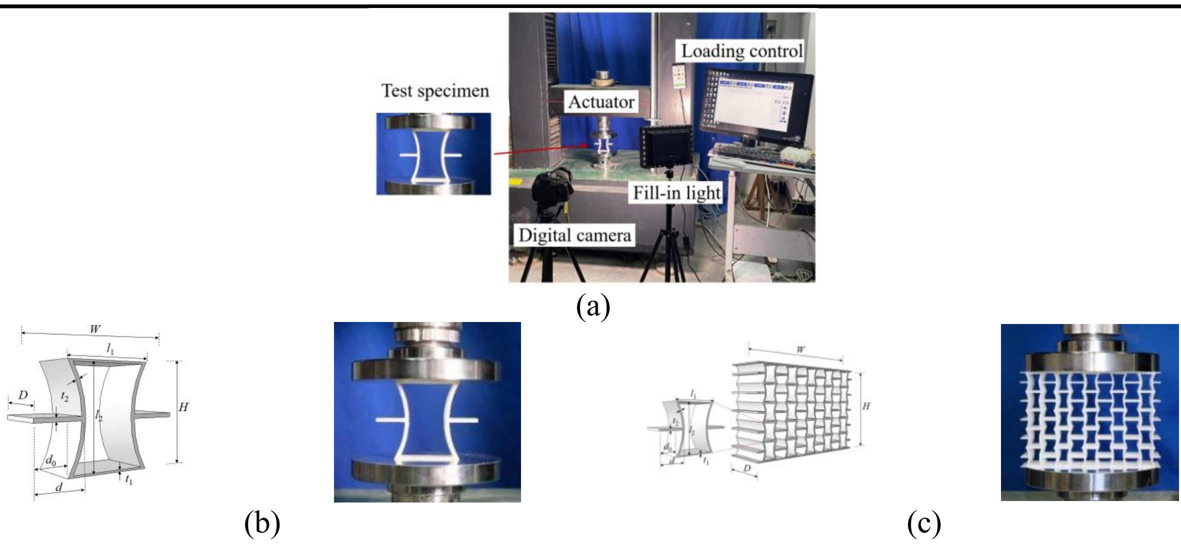

Figure 3. Geometric dimensions of uni- and multi-cellular ERH and setup for uniaxial compression **(a)** Setup for uniaxial compression; **(b)** Uni-cellular ERH; **(c)** Multi-cellular ERH.

3D finite element numerical simulations were performed in order to validate the accuracy of the 3D-EXP test. Table 2 and 3 compare displacement modes of uni- and multi-cellular ERH in the initial loading stage, beginning of compression, and at the elastic limit state obtained from test, 3D-EXP and 3D-FEM. The comparison reveals a consistent deformation mode between FE simulations and specimen tests. Specifically, the length of elliptic-arc strut within the uni-cellular ERH shortens when subjected to compression load in the non-re-entrant direction, causing inward squeezing of the elliptic-arc strut and resulting in transverse contraction. On the contrary, interactions between unit cells within the multi-cellular ERH can induce complex deformations characterized by the superposition effect of individual unit-cell deformations and stress transfer mechanisms, thereby accentuating lateral contraction deformations.

Table 2. Comparison of displacement modes of uni-cellular ERH in different stages predicted by 3D-EXP and 3D-FEM.

Models	ε_{22}=0	ε_{22}=0.013	ε_{22}=0.098
3D-EXP			
3D-FEM	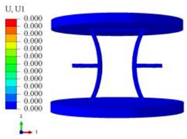	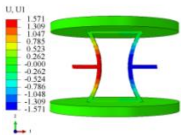	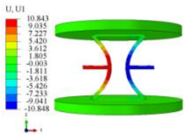

Table 3. Comparison of displacement modes of multi-cellular ERH in different stages predicted by 3D-EXP and 3D-FEM.

Models	ε_{22}=0	ε_{22}=0.018	ε_{22}=0.038
3D-EXP	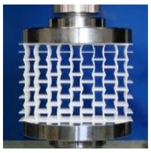	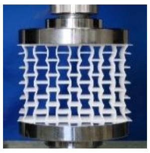	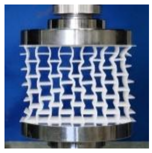
3D-FEM	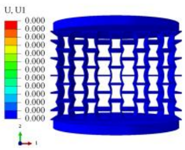	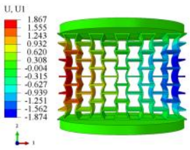	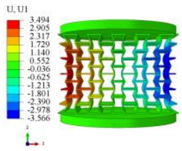

Figure 4 compares the load-displacement curves obtained from the test and 3D-FEM. The elastic moduli of uni-cellular ERH obtained from test and 3D-FEM are 20.1 MPa and 21.6 MPa, respectively. These discrepancies may stem from various factors considered in the test and simulations, such as material nonlinearity, geometric nonlinearity, contact effects, *etc.* The experimental load-displacement curve of multi-cellular ERH in Figure 4(b) exhibited an initial displacement prior to the stabilization of axial pressure, possibly attributable to non-ideal factors during the test loading process such as boundary and fixture effects, which manifested as a “concave” shape in the experimental curve. The 2-directional elastic moduli E_2 are determined by testing and 3D-FEM, resulting in values of 83.9 MPa and 79.8 MPa, respectively. The relative error for 3D-FEM compared to 3D-EXP is 4.9%. These findings suggest that the finite model is effective in predicting the compressive modulus of the ERH structure.

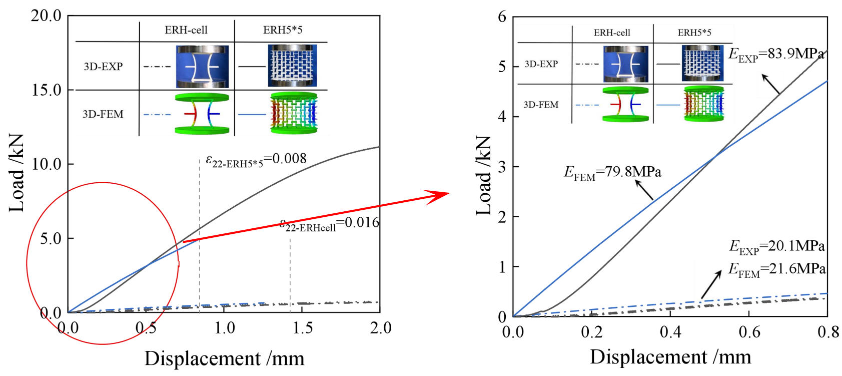

(a) (b)

Figure 4. Comparison of uniaxial compression load-displacement curves between experimental and simulates **(a)**uniaxial compression load-displacement curves; **(b)**Locally enlarged view of the linear elastic stage.

4. Performance comparison of different cellular honeycombs

4.1. Peak bearing capacity and energy absorption capacity

To compare the differences between the newly proposed ERH and the traditional structure, uniaxial compression tests were conducted on 5×5 multi-cellular ERH, ARH, and RAH using the same methodology outlined in Section 3. Examination of the experimental results in Table 4 reveals a concave deformation phenomenon on both sides of the three multi-cellular honeycombs as the axial pressure increases. This deformation characteristic confirms the negative Poisson's ratio effect observed in these multi-cellular honeycombs, where the transverse contracts instead of expands under compression, in contrast to the compressive behavior of conventional materials. The deformation of the three cellular honeycombs grows more pronounced with increasing compression, culminating in an X-shaped compression deformation. This distinctive X-shaped deformation pattern arises from the intricate deformation and plastic changes occurring within the honeycomb cells.

Figure 5 reveals that the RAH cell exhibits the highest ultimate bearing capacity, achieving 925.03 N, whereas the ARH cell displays the lowest bearing capacity at 847.43 N. The bearing capacity of the ERH cell falls between the other two, with a slight deviation of 10 N. Notably, while the ERH cell matches the load-carrying capacity of the RAH cell, its platform stage is more prolonged, indicating enhanced stability under stress, superior load distribution efficiency, and reduced deformation. In addition, the ERH cell demonstrates an energy absorption of 6.191 J and a specific energy absorption of 0.154 $J \cdot g^{-1}$, surpassing the values observed for ARH and RAH cells. This distinction highlights the ERH cell’s superior energy absorption capacity, enabling efficient energy absorption and dissipation, thereby enhancing the impact resistance of the cellular structure.

Table 4. Deformation process of different multi-cellular honeycombs under uniaxial compression.

	ε_{22}=0	ε_{22}=0.04	ε_{22}=0.08	ε_{22}=0.16	ε_{22}=0.32
Multi-cellular ERH	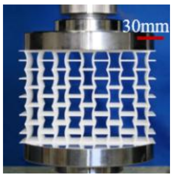	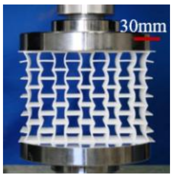	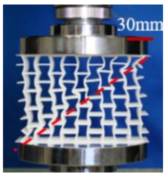	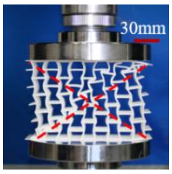	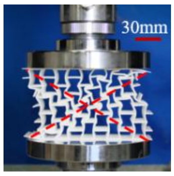
Multi-cellular ARH	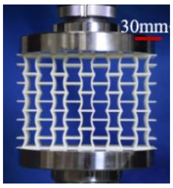	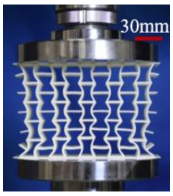	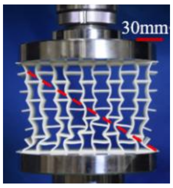	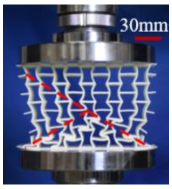	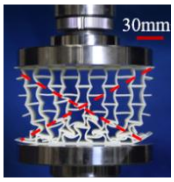
Multi-cellular RAH	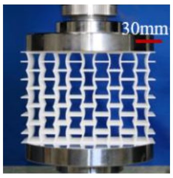	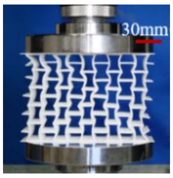	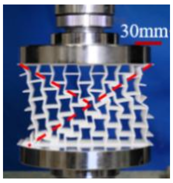	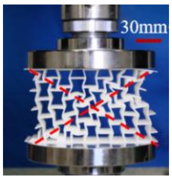	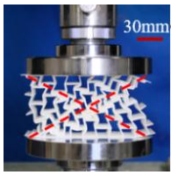

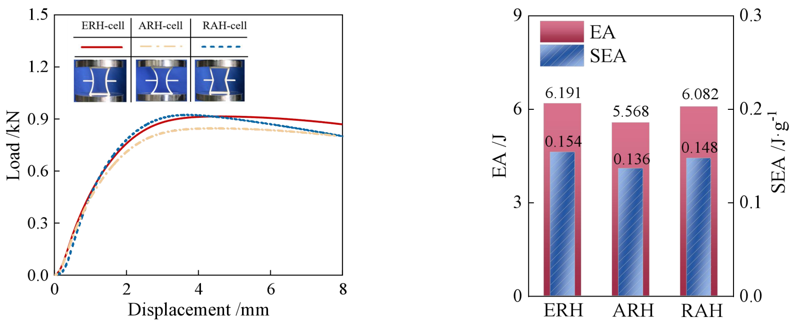

(a) (b)

Figure 5. Comparison of load-displacement curve and energy absorption capacity of uni-cellular honeycombs under uniaxial compression **(a)** load-displacement curve; **(b)** EA and SEA.

Figure 6 illustrates that ERH-5×5 exhibits the highest ultimate carrying capacity, reaching 11425.49 N, whereas ARH-5x5 demonstrates the lowest carrying capacity at 10869.34 N. Despite variations in the ultimate bearing capacity among these three cellular honeycombs, their load-displacement curves follow a similar trend. Further-more, ERH-5×5 shows an energy absorption of 29.87 J and a specific energy absorption of 0.156 J·g^{-1}, surpassing those of ARH-5×5 and RAH-5×5. This indicates that ERH-5×5 possesses superior energy absorption capabilities, enabling more effective absorption and dispersion of energy.

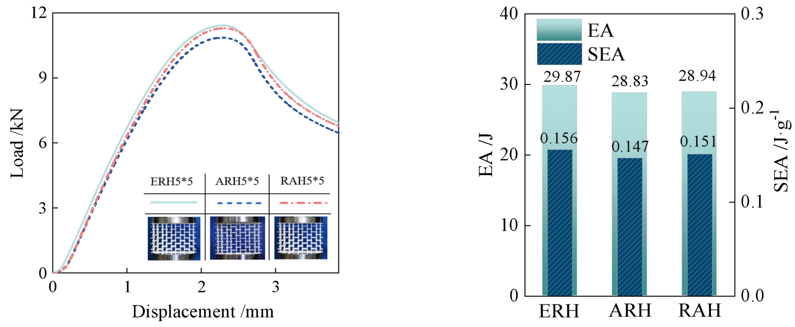

(a) (b)

Figure 6. Comparison of load-displacement curve and energy absorption capacity of 5×5 multi-cellular honeycombs under uniaxial compression **(a)** load-displacement curve; **(b)** EA and SEA.

4.2. Equivalent specific stiffness

Figure 7 compares the equivalent specific stiffness of auxetic ERH, ARH, and RAH. Minimal disparity is observed in the specific stiffness along the longitudinal direction (1-direction), whereas both ERH and RAH exhibit substantially higher lateral specific stiffness along the transverse direction (2-direction). Specifically, ERH demonstrates superior specific stiffness in the 2-direction compared to RAH. Furthermore, the sequence of decreasing shear resistance among the three honeycomb structures is RAH > ERH >ARH. In conclusion, ERH not only enhances vertical stiffness but also preserves conjugated auxeticity in the horizontal direction.

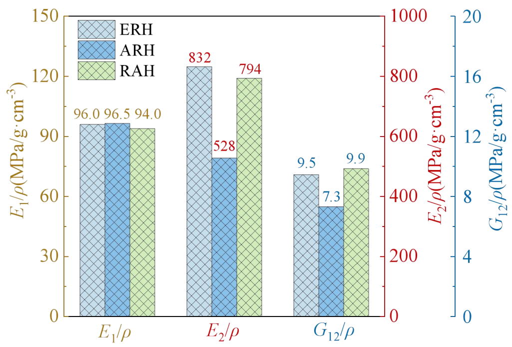

Figure 7. Comparison of equivalent specific stiffness of three re-entrant auxetic honeycomb structures.

5. Conclusions

In this study, a novel elliptic-arc re-entrant honeycomb (ERH) structure, derived from the conventional re-entrant honeycomb, is introduced. The mechanical responses of both uni- and multi-cellular structures under uni-axial compression were analyzed through a combined experimental and numerical analyses. The outcomes reveal that the ERH structure offers notable advantages in terms of load-carrying capacity, energy absorption efficiency and equivalent specific stiffness compared with multi-cellular ARH and RAH, attributable to its distinctive elliptic-arc design, thereby indicating potential practical applications.

Acknowledgement

The work described in this paper is financially supported by the National Natural Science Foundation of China (51778088, 52073036).

Conflicts of interests

The authors declare no conflict of interest.

Authors' contribution

Conceptualization and methodology, Yifeng Zhong; software and validation, Yuxin Tang; investigation, Minfang Chen; supervision, Rong Liu; review and editing, Yubo Gao. All authors have read and agreed to the published version of the manuscript.

References

[1] Qi C, Jiang F, Yang S. Advanced honeycomb designs for improving mechanical properties: a review. *Composites Part B: Engineering*. 2021, 227:109393.
[2] Greaves GN, Greer AL, Lakes RS, Rouxel T. Poisson's ratio and modern materials. *Nat. Mater.* 2011, 10(11):823–837.
[3] Zhang J, Lu G, You Z. Large deformation and energy absorption of additively manufactured auxetic materials and structures: a review. *Composites, Part B*. 2020, 201:108340.
[4] Wang Q, Li Z, Zhang Y, Cui S, Yang Z, *et al*. Ultra-low density architecture metamaterial with superior mechanical properties and energy absorption capability. *Composites, Part B*. 2020, 202:108379.
[5] Oh JH, Kim JS, Nguyen VH, Oh IK. Auxetic graphene oxide-porous foam for acoustic wave and shock energy dissipation. *Composites, Part B*. 2020, 186:107817.
[6] Wang ZG. Recent advances in novel metallic honeycomb structure. *Composites, Part B*. 2019, 166:731–741.
[7] Ren X, Das R, Tran P, Ngo TD, Xie YM. Auxetic metamaterials and structures: a review. *Smart Mater. Struct.* 2018, 27(2):023001.
[8] Peng X, Zhong YF, Shi J, Shi Z. Global buckling analysis of composite honeycomb sandwich plate with negative Poisson's ratio (OSP-RHC) using variational asymptotic equivalent model. *Compos. Struct.* 2021, 264:113721.